J. Braz. Chem. Soc., Vol. 18, No. 7, 1329-1335, 2007.
Printed in Brazil - ©2007 Sociedade Brasileira de Química
0103 - 5053 $6.00+0.00

Article

Preparation and Characterization of Carboxyl-Group Functionalized Superparamagnetic Nanoparticles and the Potential for Bio-Applications

Zhi Shan,[a] Wan-Shen Yang,[,a] Xu Zhang,[a] Qian-Ming Huang[a] and Hui Ye[b]*

[a]*Faculty of Science, Sichuan Agriculture University, Yaan 625014, Sichuan, PR China*

[b]*School of Basic Medical Science, Wenzhou Medical College, Wenzhou 325000, Zhejiang, PR China*

Neste trabalho, foi desenvolvido um método para preparação de nanopartículas magnéticas monodispersas funcionalizadas com grupos carboxila. Maguemita de dimensões nanométricas (γ-Fe_2O_3, 7,0 ± 1,0 nm) foi sintetizada usando-se o método de coprecipitação térmica e subseqüentemente coberta com grupos funcionais por copolimerização em suspensão conduzida em uma etapa. Estudos de espectroscopia de infravermelho com transformada de Fourier e análise termogravimétrica confirmaram o sucesso da funcionalização dos grupos carboxila na superfície dos nanocristais magnéticos. Esta superfície química torna possível a purificação de DNA baseada em SPRI (imobilização reversível em fase sólida). Assim, as nanopartículas foram empregadas para isolamento de DNA de cultura de células bacterianas e os resultados demonstraram sua aplicabilidade na preparação de DNA.

In this work, a method was developed to prepare monodispersed carboxyl-group functionalized magnetic nanoparticles. Nanosized maghemite (γ-Fe_2O_3, 7.0 ± 1.0 nm) was synthesized using thermal co-precipitation method and subsequently coated with functional groups by one-step suspension copolymerization. The Fourier transform infrared spectroscopy study and thermogravitmetric analyses confirmed the successful functionalization of carboxyl groups on the surface of magnetic nanocrystals. The surface chemistry makes it possible for SPRI (solid phase reversible immobilization)-based DNA purification. Thus the nanoparticles were employed to isolate plasmid DNA from bacterial cell culture and the results demonstrated its applicability in DNA preparation.

Keywords: superparamagnetic, magnetic nanoparticles, carboxyl-group, plasmid DNA

Introduction

In recent years there has been a great deal of interest with the rapid development of nanostructured materials and nanotechnology in the fields of biomedicine, including drug targeting, MRI (Magnetic Resonance Imaging) diagnosis, hyperthermia treatment of cancers and biotechnology that include detection and separation of cells, biomolecules such as proteins and nucleic acids.[1-8] Magnetite (Fe_3O_4) and maghemite (γ-Fe_2O_3) have been widely used in these cases because they are nontoxic, and with magnetic properties.[9] It is known that when the particle size is smaller than 30 nm, magnetite and maghemite particles display superparamagnetic properties, *i.e.*, they are attracted to a magnetic field but retain no magnetism after removal of magnet.[10] This property facilitates the magnetically driven separation techniques due to easy separation and dispersion of magnetic nanoparticles in solvent. The surface of the naked nanoparticles is usually tailored with synthetic or natural polymers to improve its biocompatibility and ability to be suspended in biological environment. Various functional agents such as polyethylene,[11] PEG (polyethylene glycol),[12] and silica[13] have been utilized for surface modification based on different application purposes. Besides offering grafting sites for further covalent immobilization of foreign molecules, the functional groups on the surface can be used for reversible immobilization of bio-entities.[14] The carboxyl group is one of the most promising functional groups in chemistry and biochemistry.[15] Not only are carboxyl groups readily derivatized by a variety of reactions,[16] but also they can improve the dispersion of iron oxide nanoparticles in a biological system by shifting the isoelectric point.[17,18] Carboxylated magnetic microspheres have been

*e-mail: wansheny@sicau.edu.cn

successfully used in the reversible binding of genomic DNA[19] based on SPRI technology.[20] However, it is still a technological challenge to acquire control over the nanoparticles' size and dispersibility due to attractive van der Waals or magnetic dipole-dipole interactions.[21] Nanoparticles are often found to agglomerate owing to polymer bridging mechanism or lack of steric repulsion due to inadequate polymer adsorption, which inevitably restricts its practical applications especially for *in vivo* use.[22]

Here, carboxylated superparamagnetic nanoparticles with well defined properties were synthesized. The resultant particles were nearly monodisperse without noticeable agglomeration in aqueous solution. Methacrylic acid was used as functional reagent to modify ultrafine nanocrystals. The functionalized magnetic nanoparticles were then used to elaborate a rapid protocol for extraction and purification of high quality plasmid DNA from bacteria using SPRI method. Up to 7.8 μg of plasmid DNA could be obtained from 1.5 mL of overnight culture. These nano-sized magnetic particles showed great potential in the purification of DNA towards cost-reducing, automation-friendly and simplified technology.

Experimental

Materials

All reagents were used directly as received. Analytical reagents ferric chloride 7-hydrate ($FeCl_3 \cdot 7H_2O$), ferrous sulfate 6-hydrate ($FeSO_4 \cdot 6H_2O$) and sodium hydroxide (NaOH) were purchased from Chengdu Chemical Reagent Factory (China). Benzoyl peroxide (BPO, moistured with 25% water) was purchased from Fluka (Switzerland). Methacrylic acid (MAA) of 99% purity, sodium dodecylbenesulfonate of 80% purity, trimethylolpropane triacrylate (TMPTA) of tech. grade and Bis[2-(methacryloyloxy) ethyl] phosphate (BisMEP) were all obtained from Sigma-Aldrich (USA). Ribonuclease A, sodium chloride (NaCl) and PEG8000 were purchased from Amresco (Spain). All other chemicals and solvents used in DNA isolation and analysis were of molecular biology grade. *E.coli.* strain JM109 containing pET-15b DNA (5708bp) was provided by Dr. Qi Wu. The high pure water used throughout this work was produced by Milli-Q® Biocel system (Millipore, MA, USA).

Synthesis of superparamagnetic iron oxide nanocrystals

Iron oxide nanocrystals were prepared by co-precipitating di and trivalent Fe ions in alkaline solution by a modification of previously reported method.[23] Briefly, a 100 mL solution of 4 mol L^{-1} NaOH was added to a 500 mL four neck flask equipped with a stirrer and a condenser. Then the alkali solution was bubbled with nitrogen gas (99.9% purity) for 40 min at 63 °C before an aqueous solution of Fe ions (Fe(II)/Fe(III)=1:1.65, pH 1.3), obtained by mixing 20 mL of 0.5 mol L^{-1} $FeSO_4 \cdot 6H_2O$ and 33 mL of 0.5 mol L^{-1} $FeCl_3 \cdot 7H_2O$, was quickly poured in under vigorous agitation (300 rpm). Upon introduction of Fe ions solution, a large quantity of black colloidal precipitate occurred, suggesting the formation of iron oxide. The reaction mixture was stirred for a further 90 min and then allowed to cool down at room temperature (~23 °C). The obtained nanocrystals were separated using a magnet and washed with water until the pH of supernatant was neutral. Afterward, the black precipitate was washed with absolute ethanol and acetone successively. Whereafter, a 3 days vacuum-drying treatment at room temperature was employed to completely dry the powder. A portion of resultant powder was used for characterization and the remainder for subsequent coating work.

Synthesis of carboxyl group modified magnetic nanoparticles and non-magnetic polymer particles

1.4 g synthesized iron oxide nanoparticles and 0.34 g sodium dodecyl benzenesulfonate were added in 60 mL toluene for ultrasound treatment at 800 W (Scientz-II D, Ningbo, China) for 40 min. Then another 140 mL toluene was added and the ultrasound bath continued for a further 30 min. After that, the resultant stable magnetic fluid was transferred to a four-necked 500 mL flask equipped with a condenser, thermostat and stirrer with vigorous agitation under nitrogen atmosphere (99.9% purity). At the same time, 0.4 mL of coupling agent Bis[2-(methacryloyloxy) ethyl] phosphate, 0.2 mL of cross-linking agent TMPTA, 1 mL of functional agent MAA and 0.28 g initiator BPO were introduced to the reaction system. The reaction mixture was equilibrated for at least 30 min before raising the temperature to 82 °C. The polymerization was carried out in nitrogen (99.9% purity) for 11 h, followed by cooling the reaction system to room temperature. Afterwards, the coated magnetic nanoparticles were extracted using a magnetic field and then washed successively with acetone, ethanol and high pure water to remove free monomers, residual surfactant and noxious solvents. The obtained nanoparticles were dispersed in TE solution (pH 7.2, 100 mmol L^{-1} Tris, 10 mmol L^{-1} EDTA) for subsequent plasmid DNA purification. A portion of the washed magnetic nanoparticles was dried for subsequent characterization using the same dry process as described for the uncoated iron oxide. Without adding

iron oxide nanoparticles, non-magnetic organic polymer particles (as a control) were synthesized with the same amount of reagents and the same procedures as described above.

Characterization of magnetic nanoparticles

The crystalline phase identification of the fabricated nanoparticles was obtained on a D8 Advance X-ray diffractometer (Cu Kα1 radiation, λ=1.5406 Å, Bruker-AXS, Germany), operating at 40 mA and 40 kV, with Si (SRM640) as standard sample. The average crystallite size of particles with and without coating was estimated using the Scherrer equation. The lattice parameter calculations were obtained using a least squares refinement software Unitcell. The size and morphology of magnetic nanoparticles were characterized by transmission electron microscope (TEM) using a model JEOL 100 CX II (Japan) operating at 80 kV. The size distribution was determined by measuring 1000 particles from TEM images followed by a statistical treatment. Thermal analysis was done by using a thermogravimetric analyzer (TGA, Netzsch TG209, Germany) in N_2 at a heating rate of 10 °C min^{-1}. Magnetic properties were measured by a LDJ9600 vibrating sample magnetometer (VSM, LDJ Co., USA) at room temperature. Fourier transform infrared (FTIR) spectra of the particles were performed on a Thermo Nicolet Nexus 470 spectrometer at 4 cm^{-1} resolution. The dried powder samples were applied and spread over a spectroscopic grade ~1 mm thick KBr pellet.

Plasmid DNA isolation using coated magnetic nanoparticles

Bacteria were lysed using alkaline method described elsewhere.[24] *E.coli* JM109 cells expressing the plasmid pET-15b were grown to late log phase in Luria-Bertani broth containing 50 μg mL^{-1} ampicillin. The bacterial cells were harvested from 1.5 mL of cell culture by centrifugation at 5000×g for 1 min. The pellet was re-suspended in 100 μL of 50 mmol L^{-1} Tris-HCl buffer (pH 8.0, containing 10 mmol L^{-1} EDTA and 400 μg mL^{-1} RNase A). Cell lysis was performed by gently mixing the re-suspended cells with 200 μL of 200 mmol L^{-1} NaOH containing 1% SDS (m/v). Genomic DNA and other contaminants were precipitated by addition of 150 μL of 3 mol L^{-1} potassium acetate (pH 5.5). The mixture was centrifuged at 10000×*g* for 5 min to sediment the precipitated protein, cell debris and denatured chromosomal DNA.

The supernatant of cleared alkaline lysate was placed in a 1.5 mL microcentrifuge tube. Then added $1/10^{th}$ volume of coated nanoparticles (20 mg mL^{-1}) and an equal volume of binding buffer (15% PEG8000, 2.5 mol L^{-1} NaCl). The suspension was gently mixed and placed for 1 min at room temperature (~20 °C). The particles were immobilized using a Promega™ magnetic stand and the supernatant removed. The pellet was washed twice with 750 μL of cold 70% ethanol. After immobilization of the particles, the supernatant was removed by discarding and evaporating and the plasmid DNA desorbed by addition of 50 μL of elution buffer (pH 7.8, 10 mmol L^{-1} Tris, 1 mmol L^{-1} EDTA) at room temperature for 1 min. The particles were immobilized and the supernatant transferred to a fresh DNase/RNase free microcentrifuge tube and then analyzed directly by UV spectroscopy (UV2102, Unico, China) and agarose gel electrophoresis. DNA samples were run on 0.7% agarose gel in TBE buffer (45 mmol L^{-1} boric acid, 45 mmol L^{-1} Trisbase, 1 mmol L^{-1} EDTA, pH 8.0). Gel electrophoresis experiments were carried out in three different samples, eluted supernatant, DNA/nanoparticle complex (the sample was obtained by adding 50 μL of TBE buffer instead of elution buffer, followed by quick mixing and then put to the test at once) and as comparison, plasmid DNA extracted by the Qiagen plasmid kit (Valencia, CA, USA) according to the manufacturer instruction. The bands were visualized under ultraviolet light by goldview staining, using the Gel Doc™ XR System (Bio-Rad, USA).

Results and Discussion

The X-ray diffraction patterns of the magnetic nanoparticles before and after coating respectively are shown in Figure 1. All XRD peaks could be attributed to the characteristic peaks of iron oxide spinel structure (Fe_3O_4 or γ-Fe_2O_3). The peak broadening (311) indicated that the average crystallite size of the fabricated particles

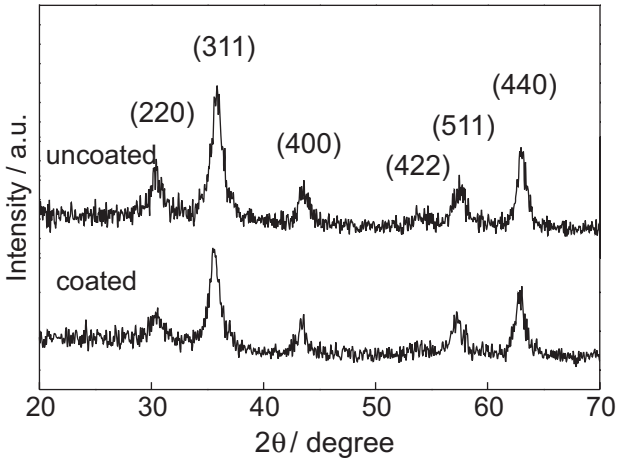

Figure 1. X-ray diffraction patterns of coated and uncoated maghemite nanoparticles.

was only a few nanometers,[25] which is ~8 nm for both samples estimated by Debye-Scherrer equation. It was noticed that the color of unmodified nanocrystals slowly changed from black to brown when exposed to air at room temperature before subsequent coating work and characterization. A similar phenomenon has been observed during the preparation of maghemite,[17] where the author stated that the nanoparticles were not chemically stable and would be oxidized to maghemite along with the diffusion of oxygen into magnetite crystallites. However, the chemical instability of magnetite nanoparticles not only results in reduced saturation magnetization, but also influences the stability of the molecular coating layer at the nanoparticle surface, thus affecting the performance for bio-applications, especially when used for photo-dynamic therapy purpose.[26] The calculated lattice parameter α was 8.3610 Å and 8.3417 Å for particles without and with coating, respectively. Since the lattice of magnetite and maghemite are 8.3960 Å (JCPDS 19-629) and 8.3515 Å (JCPDS 39-1346), respectively, the main crystalline phase of both synthesized samples could be identified as maghemite. The lattice of synthesized samples indicated partial phase transformation from magnetite to maghemite after surface modification.[17] This transformation was also confirmed by main peak shifting. The main peak (index 311) of uncoated nanoparticles was centered at 35.38°, whereas in the coated sample it was at 35.74°, this shift in the maximum was attributed to the oxidation of magnetite to maghemite as the standard 311 peaks for magnetite and maghemite were 35.423° (JCPDS 19-629) and 35.631° (JCPDS 39-1346), respectively.[27] Now that O_2 was excluded through N_2 protection during coating process, a possible explanation for phase transformation was that, before coating process, OH radical generated by ultrasonic treatment from small portion of H_2O contained in the sample and reagents induced the oxidation.[28]

A typical TEM image for the surface modified magnetic nanoparticles is shown in Figure 2 (a). It can be seen that the maghemite nanoparticles are close to spherical. The particle size distribution measured directly from TEM micrographs is shown as a histogram in Figure 2 (b). The mean particle size is 7.0 nm, with a standard deviation of 1.0 nm, which is similar to the calculated X-ray coherence length (grain size), suggesting the nanoparticles are single crystals. It can be noted that all the nanoparticles were well separated without noticeable aggregation. This reveals that the coating process did not result in significant agglomeration because of imperfect polymer coatings or different inter-polymer interaction.[29] However, it is difficult to directly observe the coating on the surface of maghemite nanoparticles from TEM micrograph. The indication of the coating formation can be obtained from TGA measurement.

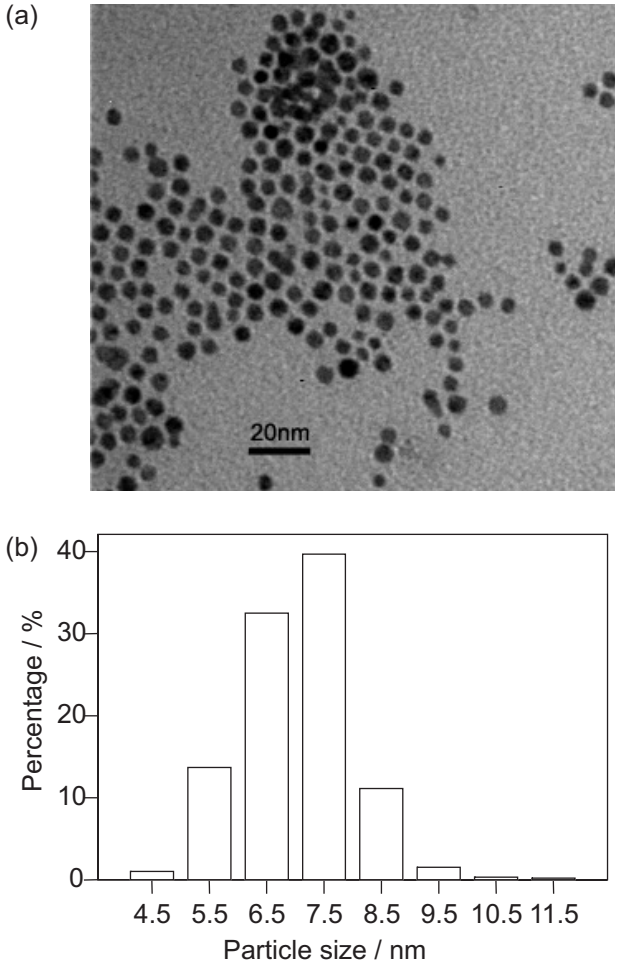

Figure 2. (a) Transmission electron microscopy (TEM) image of the coated magnetic nanoparticles. (b) Particle size distribution from TEM micrographs.

Representative FTIR spectra of maghemite nanoparticles with and without surface modification are shown in Figure 3. Compared with the naked nanoparticles, abundant absorption peaks in the spectrum of the modified particles confirmed the successful coating of polymer on iron oxide surface. The observation bands at 438 and 584 cm^{-1} in the spectrum of maghemite particles with and without coating associated with the stretching vibration mode of the Fe-O bond.[30] Further two bands around 3424 cm^{-1} and 1624 cm^{-1} ascribed to stretching and bending vibrations of surface hydroxyl groups, respectively.[31] The characteristic band in the 2850-3040 cm^{-1} frequency region originated from asymmetric and symmetric stretching modes of the C-H group also confirmed the maghemite nanoparticles were successfully coated.[32] The strong absorbance at 1724 cm^{-1} was mainly originated from the

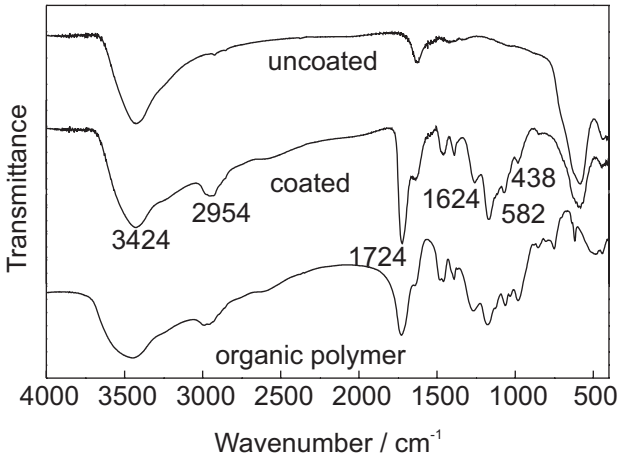

Figure 3. FTIR spectra of γ-Fe_2O_3 nanoparticles before and after coating, and organic polymer particles.

C=O vibration for the COOH groups of PMAA bound by H-bonds with oxygen atoms in the polycomplex.[33] Earlier studies by Ye's group[34] have shown that in copolymer, the C=O absorption peak of the MAA groups might split into two peaks: 1731 cm^{-1} and 1698 cm^{-1}, the 1731 cm^{-1} would be attributed to the C=O absorption peak affected by the formation of the hydrogen bonding between PMAA and PEG side chains and the 1698 cm^{-1} would be attributed to the C=O absorption peak affected by the formation of the hydrogen bonding between two carboxylic groups of PMAA on the backbone. Therefore, it was suggested the carboxyl groups in our system might exist mainly in the former mode, which was hydrogen-bonded by of OH groups of TMPTA and/or BisMEP. The spectrums for polymer coated nanoparticles and organic polymer particles are very similar, yet with a slight difference in the 400 to 800 cm^{-1} region. This difference arises from strong Fe-O bond absorbance which is a further evidence for the successful encapsulation of organic polymer on maghemite nanoparticle surface.

The plots of magnetization *versus* magnetic field (M–H loop) at room temperature for typical magnetic nanoparticles without and with surface modification are illustrated in Figure 4. Magnetic measurements indicate that both samples were superparamagnetic at room temperature, indicating that the thermal fluctuations became dominant over spontaneous magnetization at a given field,[35] and the net magnetization in the absence of an external field is zero. The magnetization value obtained at 15 kOe for uncoated particles was 54.1 emu g^{-1}, which was much lower than the value of its bulk counterpart 74 emu g^{-1} for maghemite. It is known that the saturation magnetization for single-domain superparamagnetic nanoparticles was size-dependent,[36] which could be explained by the small surface effect.[17] The surface spins of magnetic particles lack complete coordination and are likewise disordered, hence, less susceptible to changes in the strength of the external field.[37,38] This phenomenon became more significant for the nanosized particles due to their large surface-to-volume ratio. So, it was reasonable for the as-synthesized nanoparticles to have a smaller saturation value and unsaturated magnetization even under field of 15 kOe. In addition, it has been reported that the crystallinity could also affect the magnetic properties.[27] Therefore, the amorphous impurities undetectable by XRD at a grain boundary might be another reason for the diminution in the effective magnetic moment.[39] The magnetization value observed at 15 kOe for the coated magnetic nanoparticles was 47.2 emu g^{-1}, slightly lower than that for the naked ones. This was due to the mass of the polymer layer[40] and possibly, the electron exchange between the surface Fe atoms and the ligands of the polymer.[39] However, for the coated particles the specific magnetism is still strong enough to accomplish the bio-separation within 20 s using a Promega™ magnetic stand.

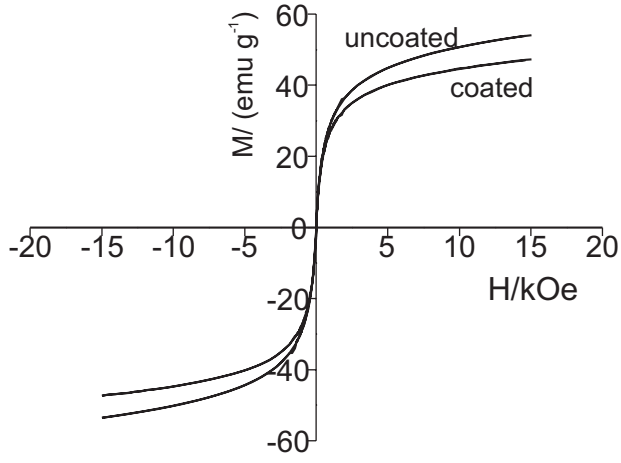

Figure 4. Room-temperature magnetization curves of the coated and uncoated maghemite nanoparticles.

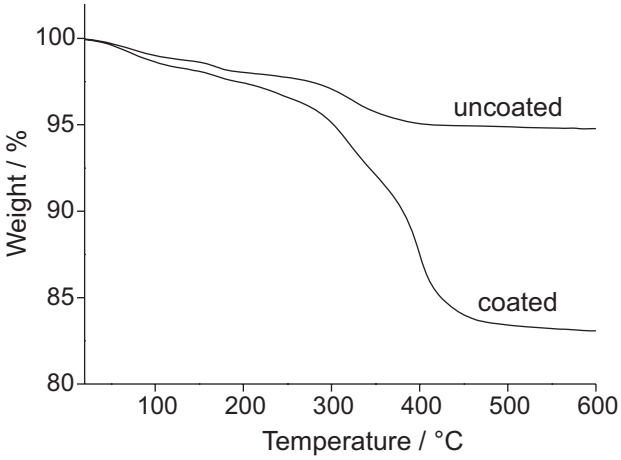

Figure 5. Thermogravimetric analysis of the magnetic nanocrystals without and with surface modification.

The TGA curves for naked and surface modified Fe_2O_3 magnetic nanoparticles are shown in Figure 5. It was noticed that there was a similar weight loss step around 300 °C for both samples. This might be due to the decomposition of amorphous iron hydroxides followed by the formation of iron oxides.[41] For naked maghemite, the initial weight loss before 250 °C could be attribute to the removal of residual water and/or surface hydroxyls, while for surface modified particles, the weight loss before 250 °C was probably due to the desorption of surface hydroxyls and/or adsorbed water and excess monomer. The significant one-step weight loss for surface modified particles occurred around 382 °C was mainly attributed to the decomposition and subsequent evaporation of coating layer.[29] In addition, the TGA curves indicated the weight loss for the coated nanoparticles was 12% higher than that of the naked one, suggesting the presence of polymer on the surface of iron oxide nanoparticles.

Figure 6 shows the agarose gel electrophoresis of plasmid DNA purified with surface carboxylated nanoparticles (lanes 3, 4, 5). With the use of only 0.8 mg nanoparticles, up to approximately 7.8 μg of high-purity (A260/A280 ratio = 1.87) plasmid DNA was isolated from 1.5 mL of overnight bacterial culture within 10 min. As comparison, plasmid DNA extracted by the Qiagen plasmid kit according to the manufacturer instruction was 6.4 μg (lane 1). Besides, the DNA/nanoparticle complex could be directly used for electrophoresis without further elution (lane 3), yet the nanoparticles stayed mainly in sample well and have no obvious negative influence on electrophoresis by comparison with lane 4. This point is very interesting for studies concentrating on sample detection as it can shorten the time from DNA preparation to electrophoresis. Further, comparison between lanes 3 and 4 indicated the high elution efficiency of plasmid DNA from functionalized nanoparticles as both bands yielded same fluorescence intensities. More importantly, in terms of the small-scale plasmid preparation, the procedure described here gain the advantage over the widely employed commercial ones using silica matrices. First, the method is of low costs but comparatively high yields. Secondly, preparations by this procedure yield a single supercoiled plasmid DNA band, as shown in Figure 6. While plasmid DNA purified by silica-based matrices is often found some type of strand-breakage during the adsorption and desorption process.[42]

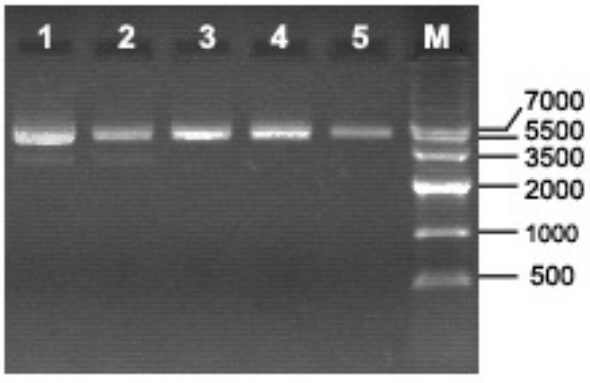

Figure 6. Agarose gel electrophoresis of plasmid DNA isolated with magnetic nanoparticles (lane 3, 4, 5) and with Qiagen plasmid kit (lane 1,2). Lane 1, 2 μL; Lane 2, 1 μL; Lane 3, 2 μL; Lane 4, 2 μL; Lane 5, 1 μL; Lane M, molecular mass marker.

Conclusions

In this paper, a method was developed to prepare well dispersed carboxylated nanoparticles with uniform properties. Maghemite nanocrystals were prepared by quick-pour-precipitation method and then these superparamagnetic crystals were modified with carboxyl groups by coating with functional agent MAA. A series of studies showed that the nanocrystals were successfully coated with well defined properties. The functionalized nanoparticles demonstrated great potential in the efficient and simple magnetic driven isolation of plasmid DNA. Starting from the preparation of bacterial lysate and ending with purified plasmids, it took less than 10 min, without the introduction of hazardous agents. Furthermore, the carboxyl moiety on the particle surface provided a binding site for the chemical immobilization of various molecules for potential specific molecular recognition.

Acknowledgments

This work was supported by the Natural Science Foundation of Sichuan Provincial Department of Education, Grant NO.2005A033. The authors would like to thank Dr. Qi Wu for the kind gift of the *E. coli.* JM109 cells.

References

1. Alexiou, C.; Arnold, W.; Klein, R. J.; Parak, F. G.; Hulin, P.; Bergemann, C.; Erhardt, W.; Wagenpfeil, S.; Lübbe, A. S.; *Cancer Res.* **2000**, *60*, 6641.
2. Weissleder, R.; Bogdanov, A.; Neuwelt, E. A.; Papisov, M.; *Adv. Drug Delivery Rev.* **1995**, *16*, 321.
3. Jordan, A.; Scholz, R.; Maier-Hauff, K.; Johannsen, M.; Wust, P.; Nadobny, J.; Schirra, H.; Schmidt, H.; Deger, S.; Loening, S.; Lanksch, W.; Felix, R.; *J. Magn. Magn. Mater.* **2001**, *225*, 118.
4. Hergt, R.; Hiergeist, R.; Hilger, I.; Kaiser, W. A.; Lapatnikov, Y.; Margel, S.; Richter, U.; *J. Magn. Magn. Mater.* **2004**, *270*, 345.

5. Lewin, M.; Carlesso, N.; Tung, C. H.; Tang, X. W.; Cory, D.; Scadden, D. T.; Weissleder, R.; *Nat.Biotechnol.* **2000**, *18*, 410.
6. Chen, D. H.; Huang, S. H.; *Process Biochem*. **2004**, *39*, 2207.
7. Yoza, B.; Arakaki, A.; Matsunaga, T.; *J. Biotechnol.* **2003**, *101*, 219.
8. Yoza, B.; Matsumoto, M.; Matsunaga, T.; *J. Biotechnol.* **2002**, *94*, 217.
9. Fu, L.; Dravid, V. P.; Klug, K.; Liu, X.; Mirkin, C. A.; *Eur. Cell. Mater.* **2002**, *3*, 156.
10. Yang, H. H,; Zhang, S. Q.; Chen, X. L.; Zhuang, Z. X.; Xu, J. G.; Wang, X. R.; *Anal. Chem.* **2004**, *76*, 1316.
11. Chatterjee, J.; Haik, Y.; Chen, C. J.; *Eur. Cell Mater.* **2002**, *3*, 98.
12. Zhang, Y.; Kohler, N.; Zhang, M.; *Biomaterials* **2002**, *23*, 1553.
13. Klug, K. L.; Dravid, V. P.; Johnson, D. L.; *J. Mater. Res*. **2003**, *18*, 988.
14. Chiang, C. L.; Sung, C. S.; Wu, T. F.; Chen, C.Y.; Hsu, C.Y.; *J. Chromatogr., B* **2005**, *822*, 54.
15. Morais, P. C.; Santos, R. L.; Pimenta, A. C. M.; Azevedo, R. B.; Lima, E. C. D.; *Thin Solid Films* **2006**, 515, 266.
16. Wong, S. S.; Joselevich, E.; Woolley, A. T.; Cheung, C. L.; Lieber, C. M.; *Nature* **1998**, *394*, 52.
17. Yu, S.; Chow, G. M.; *J. Mater. Chem.* **2004**, *14*, 2781.
18. Durgin, P. B.; Chaney, J. G.; *Can. J. Soil. Sci.* **1984**, *64*, 445.
19. Krížová, J.; Španová, A.; Rittich, B.; Horák, D.; *J. Chromatogr., A* **2005**, *1064*, 247.
20. Hawkins, T. L.; O'Connor-Morin, T.; Roy, A.; Santillan, C.; *Nucleic Acids Res*. **1994**, *22*, 4543.
21. Puntes, V. F.; Krishnan, K. M.; Alivisatos, P.; *Appl. Phys. Lett.* **2001**, *78*, 2187.
22. Tartaj, P.; Morales, M. del Puerto; Veintemillas-Verdaguer, S.; González-Carreño, T.; Serna, C. J.; *J. Phys. D: Appl. Phys.* **2003**, *36*, R182.
23. Xie, X.; Zhang, X.; Zhang, H.; Chen, D.; Fei, W.Y.; *J. Magn. Magn. Mater.* **2004**, *277*, 16.
24. Levison, P. R.; Badger, S. E.; Dennis, J.; Hathi, P.; Davies, M. J.; Bruce, I. J.; Schimkat, D.; *J. Chromatogr., A* **1998**, *816*, 107.
25. Mikhaylova, M.; Jo, Y. S.; Kim, D. K.; Bobrysheva, N.; Andersson, Y.; Eriksson, T. ; Osmolowsky, M.; Semenov, V.; Muhammed, M.; *Hyperfine Interact.* **2004**, *156/157*, 257.
26. Silva, S. W. da; Melo, T. F. O.; Soler, M. A. G.; Lima, E. C. D.; Silva, M. F. da; Morais, P. C.; *IEEE Trans. Magn.* **2003**, *39*, 2645.
27. Feltin, N.; Pileni, M. P.; *Langmuir* **1997**, *13*, 3927.
28. Yang, C.; Wang, G.; Lu, Z.; Sun, J.; Zhuang J.; Yang, W.; *J. Mater. Chem.* **2005**, *15*, 4252.
29. Sahoo, Y.; Pizem, H.; Fried, T.; Golodnitsky, D.; Burstein, L.; Sukenik, C. N.; Markovich, G.; *Langmuir* **2001**, *17*, 7907.
30. Barrón, V.; Torrent, J.; Grave, E. de; *Am. Mineral*. **2003**, *88*, 1679.
31. Mikhlin, Yu. L.; Kuklinskiy, A. V.; Pavlenko, N. I.; Varnek, V. A.; Asanov, I. P.; Okotrub, A. V.; Selyutin, G. E.; Solovyev, L. A.; *Geochim. Cosmochim. Acta* **2002**, *66*, 4057.
32. Tannenbaum, R.; King, S.; Lecy, J.; Tirrell, M.; Potts, L.; *Langmuir* **2004**, *20*, 4507.
33. Polacco, G.; Cascone, M. G.; Petarca, L.; Peretti, A.; *Eur. Polym. J.* **2000**, *36*, 2541.
34. Ye, M.; Zhang, D.; Han, L.; Tejada, J.; Ortiz, C.; *Soft Matter* **2006**, *2*, 243.
35. Sun, S.; Zeng, H.; Robinson, D. B.; Raoux, S.; Rice, P. M.; Wang, S. X.; Li, G.; *J. Am. Chem. Soc.* **2004**, *126*, 273.
36. Liu, C.; Rondinone, A. J.; Zhang, Z. J.; *Pure Appl. Chem.* **2000**, *72*, 37.
37. Kachkachi, H.; Ezzir, A.; Noguès, M.; Tronc, E.; *Eur. Phys. J. B* **2000**, *14*, 681.
38. Kodama, R. H.; Berkowitz, A. E.; McNiff, E. J. Jr.; Foner, S.; *Phys. Rev. Lett.* **1996**, *77*, 394.
39. Liao, M. H.; Chen, D. H.; *J. Mater. Chem.* **2002**, *12*, 3654.
40. Fu, L.; Dravid, V. P.; Johnson, D. L.; *Appl. Surf. Sci.* **2001**, *181*, 173.
41. Yen, F. S.; Chen, W. C.; Yang, J. M.; Hong, C. T.; *Nano Lett.* **2002**, *2*, 245.
42. Li, Y.; Knobloch, O.; Hahn, H. P.; *J. Biochem. Biophys. Methods* **2002**, *51*, 69.

Received: March 8, 2007
Web Release Date: October 31, 2007